Available online at www.sciencedirect.com
SCIENCE DIRECT®
Physics and Chemistry of the Earth 29 (2004) 241–249
PHYSICS and CHEMISTRY of the EARTH
www.elsevier.com/locate/pce

Global distributions of the refraction index variances at different altitudes in the atmosphere from GPS/MET satellite occultation data

N.M. Gavrilov [a,*], N.V. Karpova [a], Ch. Jacobi [b]

[a] Department of Atmospheric Physics, Saint-Petersburg University, 1 Ul'yanovskaya Street, Petrodvorets, Saint Petersburg 198504, Russian Federation
[b] Institute for Meteorology, University of Leipzig, 3 Stephanstrasse, 04103 Leipzig, Germany

Abstract

The GPS/MET satellite measurements during years 1995–1997 at altitudes 2–35 km are used to obtain global distributions of meso-scale variances of the refraction index (''dry temperature'') at different stratospheric altitudes. Individual dry temperature profiles are smoothed using second order polynomial approximations in 7 km thick layers centered at 2, 5, 10, 15, 20, 25, 30 and 35 km. Refraction index deviations from smoothed values and their variances are obtained for each profile and are averaged for each month of the year during the GPS/MET experiment. Global distributions of dry temperature variances have inhomogeneous structure. Locations and latitude distributions of the variance maxima and minima depend on altitudes and months of year. The reasons for the small- and meso-scale refraction index perturbations in the tropo–stratosphere could be meso-scale irregularities, turbulence and internal gravity waves. Magnitudes of the refraction index variances are larger in the regions of tropo–stratrospheric jet streams and of equatorial deep convection.

Keywords: Middle atmosphere dynamics; Waves and turbulence; Climatology; Global positioning system; Satellites; Radio occultation

1. Introduction

An important problem of atmospheric dynamics (especially for the middle and upper atmosphere) is the study of generation and propagation of wave motions and their influence on the general circulation, thermal regime and composition of the atmosphere. Observations show that wave processes are important components of dynamic processes at all altitudes. In this connection, an increased attention is given to their studies recently. According to common view, it is not possible to develop adequate theories of thermal regime, circulation, gas and ion composition of the mesosphere and thermosphere without taking account of the influence of wave processes (Fritts and Alexander, 2003). Important sources of atmospheric waves of different scales are meteorological and turbulent processes (winds in the mountains, cyclones, meso- and small-scale vortexes, fronts, jet streams, etc.).

Several recent studies were devoted to geographical structure of internal gravity waves (IGWs) in the atmosphere. Allen and Vincent (1995) and Hirota (1984) made the analysis of high-resolution data from radiosondes. Eckermann et al. (1995) analyzed rocket measurements. New satellite-borne remote sensing measurements provide excellent global information on the background dynamical structure, planetary-scale fluctuations, and meso-scale disturbances. Fetzer and Gille (1994) used satellite data from the Limb Infrared Monitor of the Stratosphere (LIMS). Eckermann and Preusse (1999) presented results from Cryogenic Infrared Spectrometer and Telescopes for the Atmosphere (CRISTA). Wu and Waters (1996) and McLandress et al. (2000) extracted temperature fluctuations with horizontal scales less than 100 km, and studied a global distribution of gravity wave activity in the stratosphere and mesosphere (30–80 km) using data from the Microwave Limb Sounder (MLS) on board of the UARS satellite. Alexander (1998) explained the UARS-MLS results with a

* Corresponding author. Tel.: +7-812-428 4489; fax: +7-812-428-7240.
E-mail address: gavrilov@pobox.spbu.ru (N.M. Gavrilov).

1474-7065/$ - see front matter © 2004 Published by Elsevier Ltd.
doi:10.1016/j.pce.2004.01.006

numerical model assuming globally uniform IGW excitation in the troposphere.

Owing to these intensive observational and theoretical studies, our knowledge of the IGW behaviour has greatly advanced during the last decade. Yet, the global distribution of IGW activity is not well defined; better definition is needed to fully understand and model wave effects according to geographic and seasonal conditions. In particular, little is known about simultaneous global structure of IGW in the middle atmosphere and TIDs in the ionosphere.

The Global Positioning System/Meteorology (GPS/MET) experiments have been performed by the University Corporation for Atmospheric Research (UCAR), which provided a global high resolution data set of temperature, pressure and refractivity profiles in the stratosphere. In this experiment a GPS receiver aboard MicroLab-1 satellite was launched on April 3, 1995, into a low earth orbit (LEO) to observe occulted radio signals from GPS satellites. Height profiles of atmospheric refractive index were derived from these observations and stratospheric temperature was obtained using a technique described by Ware et al. (1996) and Rocken et al. (1997). These data show 1 °C mean temperature agreement with meteorological data between 5 and 40 km altitude. Tsuda et al. (2000) made the first analysis of global morphology of IGW activity in the stratosphere from GPS/MET data. This study has shown that the LEO/GPS occultation technique provides important and unique data for studies of the global distribution of atmospheric IGWs.

However, this study was restricted to stratospheric altitudes, where variations of the atmospheric refraction index depend mainly on perturbations of temperature and density. At lower altitudes, atmospheric humidity gives an important contribution into the refraction index fluctuations, which hampers interpretation. Therefore, in the interpretation of LEO/GPS satellite data, the use of the refraction index perturbations themselves seems to be more convenient for qualitative study of locations of the zones of increased meso-scale variability in the tropo–stratosphere. Wu et al. (2002) used the refraction index perturbations measured with CHAMP LEO/GPS satellite to find the dynamically active zones in the stratosphere and ionosphere.

The objective of the present study is the statistical analysis of meso-scale variability of the refraction index to find global distributions of dynamically active zones at different altitudes in the tropo–stratosphere.

2. Radio wave refraction index

Radio occultations have been used for the past 30 years to explore the atmospheres of different planets. The technique has been an important part in the NASA programme for solar system exploration. Typically, a spacecraft transmitter is linked to a terrestrial or other spacecraft receiver via cm-wavelength radio signals. When the propagation path from the transmitter to the receiver passes through the planetary atmosphere, the signal is slowed and bent on its way through the atmosphere. The delay can be measured, the inversion of its time derivative yields atmospheric refraction index as a function of height.

On April 3rd, 1995, the MicroLab-1 satellite was launched, marking the start of the GPS/MET experiment. Until March 1997, the satellite GPS receiver was operated. The research satellite orbited the Earth between 730–750 km altitudes with a period of 100 min. It was 70° inclined and carried a laptop-sized radio receiver whose antenna pointed in the negative direction of flight (Ware et al., 1996; Rocken et al., 1997). Hence, the satellite could only observe rising or setting occultations, not both simultaneously. Under optimum conditions, about 150 soundings at different latitudes and altitudes were collected by the GPS/MET instrument per day. The GPS/MET satellite data have been processed and are available via the Internet. The satellite gives vertical profiles of radio wave refraction index at heights 5–60 km with heigh resolution of 0.2 km. The refraction index, n, or refractivity, N, is related to atmospheric parameters by the following expression (Kursinski et al., 1997):

$$N = (n-1)\times 10^6 = 77.6\frac{p}{T} + 3.73\times 10^5\frac{e}{T^2} + 4.03\times 10^7\frac{N_e}{f^2}, \quad (1)$$

where p is atmospheric pressure [hPa], T is atmospheric temperature [K], e is water vapor partial pressure [hPa], N_e is electron number density [m^{-3}], f is the radio wave frequency [Hz]. Generally, N decreases exponentially, like $\exp(-z/H)$ with increasing altitude. This fast decrease makes it difficult to evaluate small deviations of the refraction index directly from its height profiles. More sensitive to small variations is the so-called "dry temperature", which usually is obtained using the expression

$$T_{\mathrm{dry}} = 77.6p/N. \quad (2)$$

The dry temperature is a good estimation of atmospheric temperature at altitudes 15–30 km. Below 15 km, the humidity terms in (1) become substantial and the approximation of dry temperature does not reflect real atmospheric temperature. Above 30–35 km the errors of eliminating ionospheric contribution become comparable with the dry temperature term in (1). Dynamical processes in the atmosphere lead to the variations δp and δT of parameters in (1). For small-scale turbulence and low-frequency short internal gravity waves (IGWs) usually $|\delta p/p| \ll |\delta T/T|$ (Monin and Yaglom, 1971; Hines, 1960). Therefore, from (2) we can get

$$|\delta N/N| = |\delta T_{\mathrm{dry}}/T_{\mathrm{dry}}|. \quad (3)$$

Therefore, variances of dry temperature reflect the variances of refractivity at all altitudes. This was confirmed by direct comparison of the refraction index and dry temperature variances from GPS/MET data by Gavrilov et al. (2004). As a measure of the refraction index variances in the present paper we use the variances of the dry temperature. Wu et al. (2002) for the analysis of CHAMP GPS satellite data tried to use vertical profiles of the refraction index variances. These profiles visually show substantially smaller meso-scale variations compared to the dry temperature profiles. Gavrilov et al. (2004) showed that this difference is due to the fast exponential decrease of refractivity in altitude, and proper approximation and subtraction of the mean refractivity and dry temperature profiles reveals good validity of (3).

3. Method of statistical analysis

The methods of retrieving the dry temperature from GPS/MET data are described by Rocken et al. (1997) and Tsuda et al. (2000). For the GPS/MET experiment, the height step of the data presentation is $\Delta z = 0.2$ km. Tsuda et al. (2000), analyzing IGWs from GPS/MET data, used an approximation of temperature vertical profiles with a smooth mathematical function and calculated deviations from these smooth profiles. From the variety of possible mathematical functions for smoothing, the polynomial ones are frequently used for the analysis of radiosonde and satellite vertical profiles of atmospheric parameters. There are two parameters: the power of the polynomial and the thickness of the height layer, δz, for approximation, which can influence the quality of the approximation. Therefore, we analyze first the possible impact of these parameters on the approximation of temperature profiles in Section 3.1. According to Ware et al. (1996), the theoretical temperature accuracy is better than 0.5 K near the tropopause, degrading to about 1 K at 40 km altitude.

3.1. Polynomial fits

Fig. 1 shows examples of approximation of GPS/MET dry temperature profiles with polynomial fits of the second power within different height fitting layers of thicknesses $\delta z = 5$ and 10 km. One can see that the increase in δz leads to deterioration in the fit of the data. Right parts of plots at Fig. 1 show deviations of observed dry temperature values from the polynomial fits. Based on these results, we used the thickness of the height layer $\delta z \sim 7$–10 km. A comparison of the second and third power polynomial approximation shows that the cubic approximation gives practically the same results as the quadratic one. Therefore, the quadratic approximation seems to be sufficient for the fitting of GPS satellite dry temperature data in the stratosphere.

To estimate possible errors from polynomial fitting the GPS satellite data, we made approximation of MSISE-90 model (Hedin, 1991) temperature profiles at different latitudes with quadratic polynomial fits. We estimated variances of relative deviations of temperature from the polynomial fit:

$$\delta T/T_0 = \sqrt{\frac{1}{N}\sum_{i=1}^{N}\left(\frac{T_i - T_{i0}}{T_{i0}}\right)^2}, \quad (4)$$

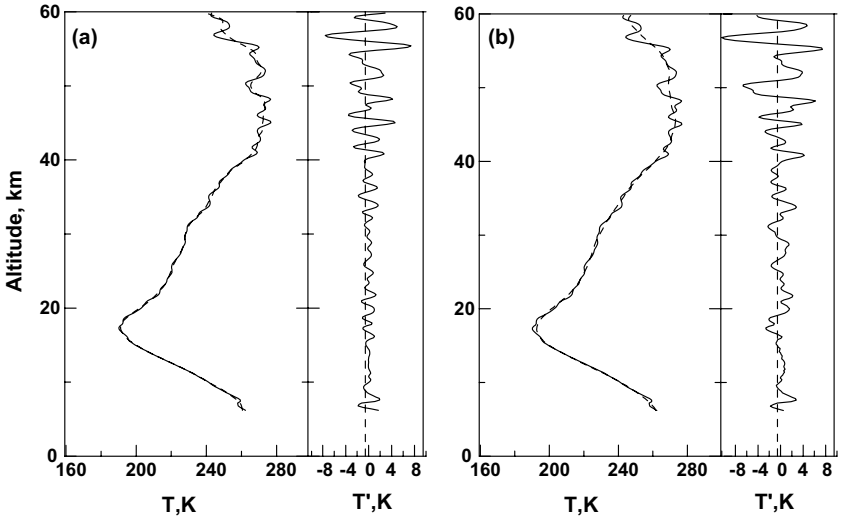

Fig. 1. An example of dry temperature measured with GPS/MET satellite (solid lines) and running quadratic polynomial approximation (dashed lines) with height intervals for approximation of: (a) 5 km and (b) 10 km. Deviations from the approximations are shown at right sections of the plots.

where T_i and T_{i0} are the model and approximated temperature values, respectively, N is the number of values containing within height layer of thickness δz centered at altitude z_0. Results of estimations of variances of the deviations between MSISE-90 model and approximated temperature profiles show that errors from quadratic fitting of the GPS satellite temperature data generally increase with the increase in height layer thickness δz. Values of variances of 2×10^{-4}–2×10^{-2} for $\delta z = 5$–10 km, respectively, are smaller than the observed natural variances of stratospheric temperature caused by atmospheric dynamical processes.

3.2. Instrumental noise

Above mentioned studies by Ware et al. (1996) and Rocken et al. (1997) estimate the discrepancies between the average temperature profiles obtained with GPS/MET satellite and radiosondes. These discrepancies depend not only on the accuracy of observations, but also on the level of atmospheric turbulent and wave noise. Nevertheless, to evaluate possibilities of GPS satellite data for study of meso-scale perturbations in the atmosphere, it is essential to estimate the level of random noise in the data, which may be caused by the instrumental errors and methodical inconsistencies during the dry temperature retrieval from the data. Influence of random instrumental errors in the data can be estimated using the temperature structure function versus altitude:

$$D(\mathrm{d}z) = \langle [T(z+\mathrm{d}z) - T(z)]^2 \rangle \quad (5)$$

where $\mathrm{d}z$ is the height difference, $\langle\ \rangle$ denote averaging over fitting height layer. If experimental data contain random instrumental errors with variance D_{err}, then $\lim_{\mathrm{d}z\to 0} D(\mathrm{d}z) = 2D_{\mathrm{err}}$ (see Gavrilov et al., 1994). Fig. 2 represents examples of height structure functions for GPS/MET data at different height layers. One can see that in all cases the structure functions at smallest possible $\mathrm{d}z = 0.2$ km are smaller than that at larger $\mathrm{d}z$. This can give additional evidences that the level of instrumental noise in GPS/MET data is substantially smaller than the natural temperature variability in the stratosphere.

3.3. Approach

In the present analysis we select data for $\delta z = 7$ km thick layers centered at altitudes 2, 5, 10, 15, 20, 25, 30 and 35 km. For most cases, this gives 1 km overlap between consecutive layers, which may give some correlation of the results. However, this correlation is expected to be small, also smaller separation between the layer centers gives better representation of vertical changes in the refraction index variances. For each vertical profile of dry temperature measured with GPS/MET satellite, we make quadratic approximation for smoothing temperature inside each layer. Then we calculate variances of temperature deviations from the smoothed values inside each layer. Afterwards, we select groups of these variances for respective months during GPS/MET experiment from 1995 to 1997. To get latitude-longitude distributions, the data for each layer were interpolated to a regular grid using weighted averaging over circles with radii of 8° in latitude and longitude centered at each grid point. In most cases, we had 8–15 data points for interpolation within these circles.

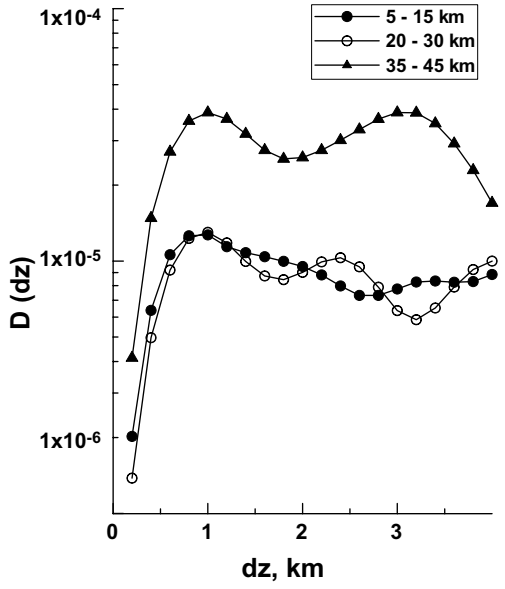

Fig. 2. Examples of GPS/MET dry temperature structure functions for altitude layers: (filled circles) 5–15 km; (open circles) 20–30 km and (triangles) 35–45 km.

4. Results of the analysis

Fig. 3 shows latitude-longitude distributions of the refractive index variances at different height layers averaged over January. At altitude 15 km, where the dry temperature (2) is good approximation to the real atmospheric temperature, one can see the band of increased temperature variances between latitudes ±20–30°. The same band was observed by Tsuda et al. (2000). At altitudes 20–25 km in Fig. 3 the tropical convection band become narrower and weaker and one can see increased dry temperature variations near North Pole. At 30–35 km the zones of higher refraction index variances are spread around the middle and low latitudes with some dominance in the northern hemisphere in January (see Fig. 3).

Observed in Fig. 3 distributions of dry temperature variances above altitudes 15 km are generally the same

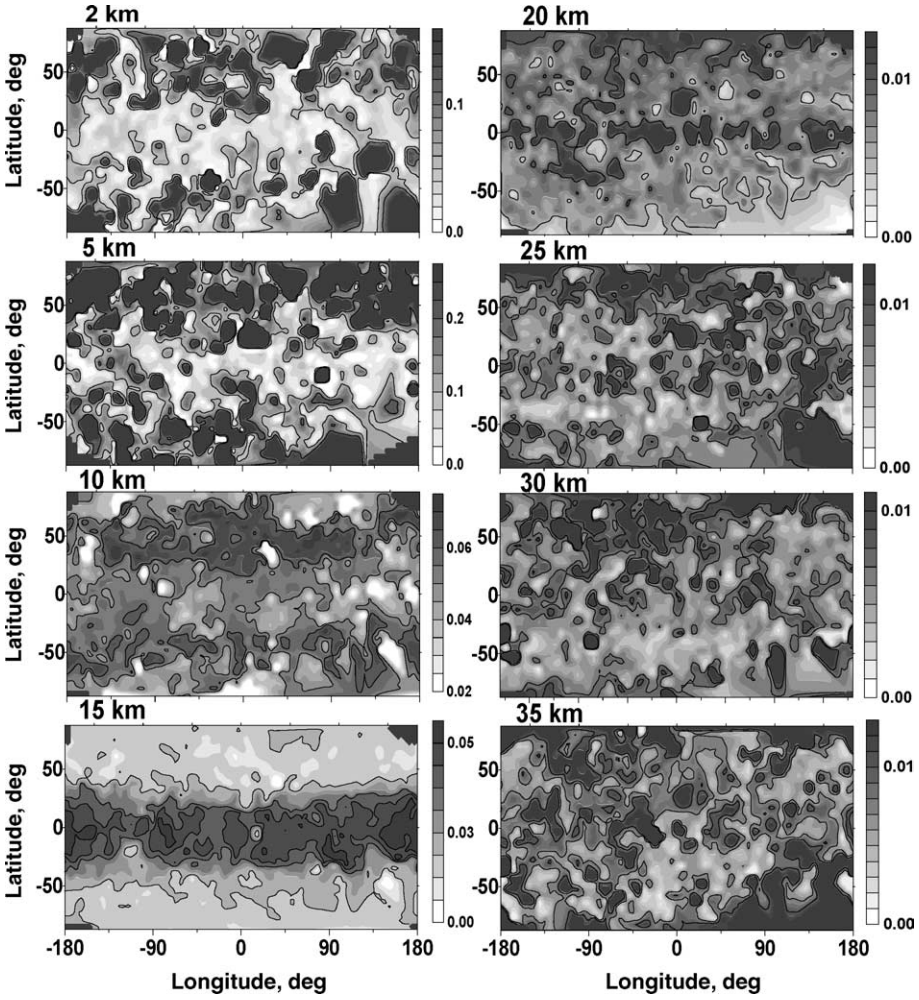

Fig. 3. Average over years 1995–1997 latitude–longitude distributions of the refraction index relative variances from GPS/MET satellite data for different altitude layers in January. Numbers above the plots show altitudes in km.

as were found by Tsuda et al. (2000) from GPS/MET data. Below 15 km the dry temperature is not a good approximation to the atmospheric temperature but reflects the variations of the atmospheric refraction index (see Gavrilov et al., 2004). Due to big variability of individual dry temperature variances and limited number of data points for interpolating at every grid points (see Section 3.3), the distributions in Fig. 3 are not smooth enough. Therefore, one may analyze only general structures of the variance distributions in Fig. 3 and afterwards.

Considered from this point of view, the distributions of dry temperature variances presented at plots of Fig. 3 for altitudes 2 and 5 km show generally larger variances at latitudes higher ±(20–30°) in both hemispheres with predominance of variances in the northern hemisphere in January. In the height layer centered at 10 km in Fig. 3, one can see the bands of increased dry temperature variances in the middle latitudes of both hemispheres centered near latitudes ±50° with larger magnitudes in the northern hemisphere. These bands may reflect increased generation of meso-scale irregularities inside tropo–stratospheric jet streams (see discussion in Section 5).

In Fig. 5 for July one can see the latitude–longitude distributions at all altitudes to be similar to the January distributions seen in Fig. 3. At altitudes 2 and 5 km there are zones of increased refraction index variances at middle and high latitudes. The bands associated with jet streams near latitudes ±50° and with tropical convection centered at the equator exist in Fig. 5 at altitude 10 km. At altitudes 20–25 km one can see zones of increased refraction index variances at high latitudes of southern hemisphere in July. At altitudes 30–35 km in July, Fig. 5 show dispersed zones of increased dry temperature variances located mainly in southern hemisphere instead of the northern hemisphere in January.

Figs. 4 and 6 are similar to Figs. 3 and 5, but for April and October, respectively. The latitude–longitude distributions of the refraction index variances in equinoxes have the same main structures as the solstice distributions. The main difference is more symmetric distributions

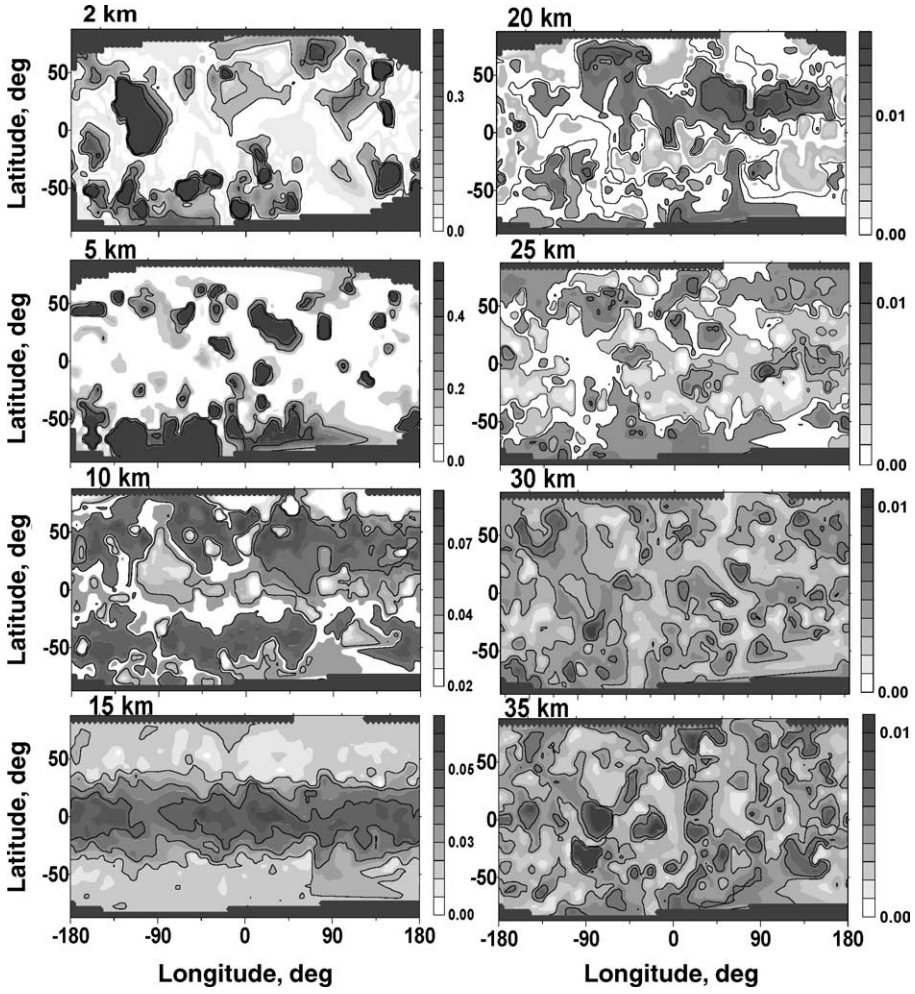

Fig. 4. Same as Fig. 3, but for April. Rectangular black areas near the poles show the regions without the data points.

of the variances at altitudes 30–35 km between the northern and southern hemispheres at equinoxes in Figs. 4 and 6, than that at solstice in Figs. 3 and 5.

5. Discussion

Variations of the refraction index in the atmosphere may be produced by dynamical processes, which could make inhomogeneities of density, temperature, humidity and electron density. In the stratosphere, the main reason for the refraction index variance is temperature change. The method of analysis described in Section 2 estimates the variances caused by small- and meso-scale inhomogeneities with vertical scales up to the fitting layer thickness of $\ddot{a}z \sim 7$–10 km. Such variations may be produced by meso-scale turbulent and wave processes in the atmosphere. Figs. 3–6 show large magnitudes of refraction index variances in the troposphere below altitude of 15 km. Amplitudes of meso-scale atmospheric waves in the troposphere are normally relatively small. Therefore, the reasons for substantial variances of the refraction index observing in Figs. 3–6 could be meso-meteorological and convective processes forming meso-scale turbulence in the troposphere.

At low altitudes 2–5 km the reasons for the meso-scale variances could be interactions of atmospheric winds with mountain systems, boundary layer convection and inhomogeneous solar heating due to irregular distributions of water vapor. Near 10–12 km the maxima of tropospheric planetary jets exist. Instability of the tropospheric jets may produce the midlatitude bands of increased variances of refraction index seen at altitude 10 km in Figs. 3–6. Meso-scale turbulence in the tropo–stratospheric jet streams may generate IGWs propagating to the middle atmosphere. Gavrilov et al. (1999) used Japanese MU radar measurements to estimate intensities of meso-scale turbulent dynamical sources in the atmosphere. They found the strength of such sources to increase with the mean wind velocity. A correlation of perturbed zones in the atmosphere with the mean wind speed was obtained also by McLandress et al. (2000) from the analysis of the Microwave Limb Sounder satellite data.

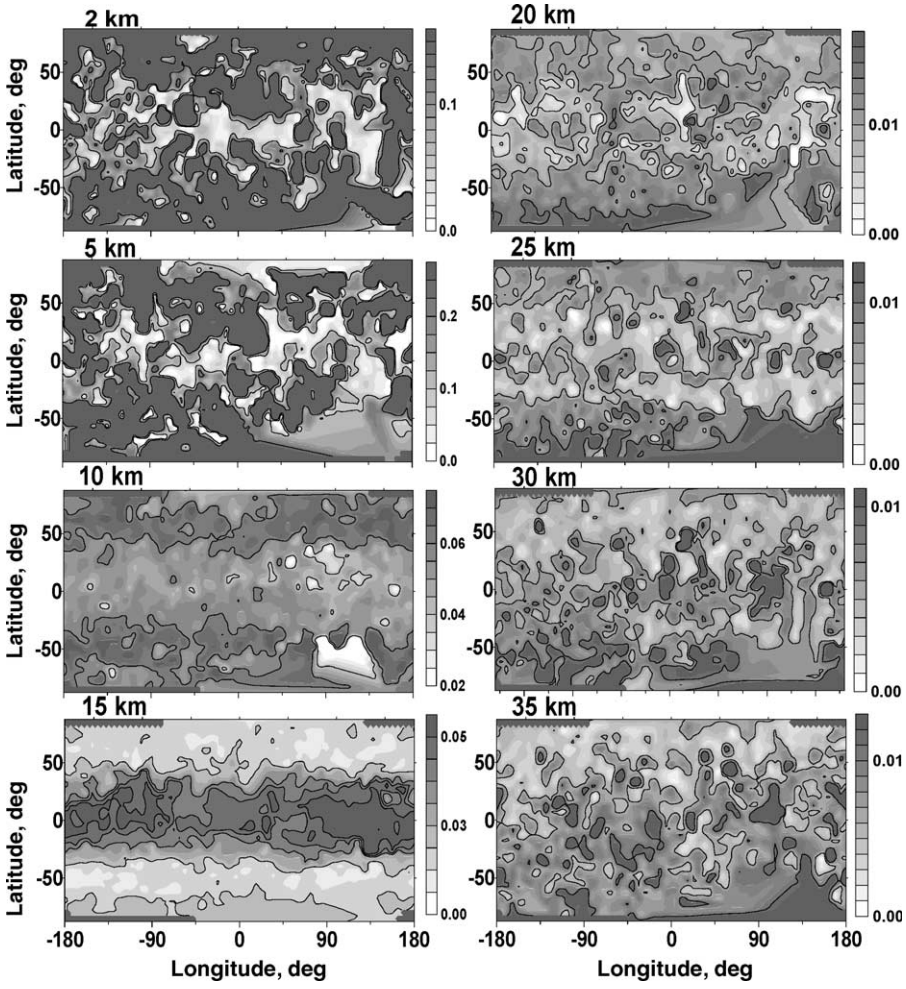

Fig. 5. Same as Fig. 3, but for July.

At altitudes 15–20 km there is intensive deep convection in tropical region, which may be seen in Figs. 3–6. Alexander et al. (2002) supposed that the layer of increased dry temperature variances observed with GPS/MET satellite may be caused by a decrease in the Coriolis parameter near the equator, leading to the widening of frequency band allowed for IGWs in the atmosphere. At the same time, one should keep in mind that at altitudes 15–18 km certain contribution into meso-scale variations of the refraction index might give convective irregularities in tropical cloud systems extending up to the tropopause. The intensity of convective processes is assumed to have a maximum near the equator. Therefore, the irregularities produced by this deep convection together with IGWs, which can be generated by this convection (Alexander, 1996), may produce a band of increased refraction index variances near the equator at altitudes of 15–20 km in Figs. 3–6.

Orographic processes, convection and meso-scale turbulence produced in the jet streams may generate meso-scale IGWs propagating into the middle atmosphere. Above altitude of 25 km in Figs. 3–6 variances caused by meso-scale turbulence are expected to become smaller and we could more clearly observe IGWs propagating to the stratosphere from below. IGW amplitudes increase with height due to decrease in atmospheric density and the refraction index variances begin to grow after altitude 25 km in Figs. 3–6. Lager variances in the northern hemisphere in January and in the southern hemisphere in July may be explained by the influence of background wind and temperature on the IGW propagation in the middle atmosphere. Such influence may suppress IGW amplitudes in summer hemisphere and to increase the amplitudes in winter hemisphere.

On the other hand, consideration of Figs. 3–6 shows quit good consistency of the results for the same altitudes in different seasons, which is unlikely caused by random instrumental noise. Therefore, we may expect that estimations of meso-scale variances of the dry temperature/refraction index from LEO/GPS satellite data may give at least qualitative information about global distributions of dynamically disturbed regions,

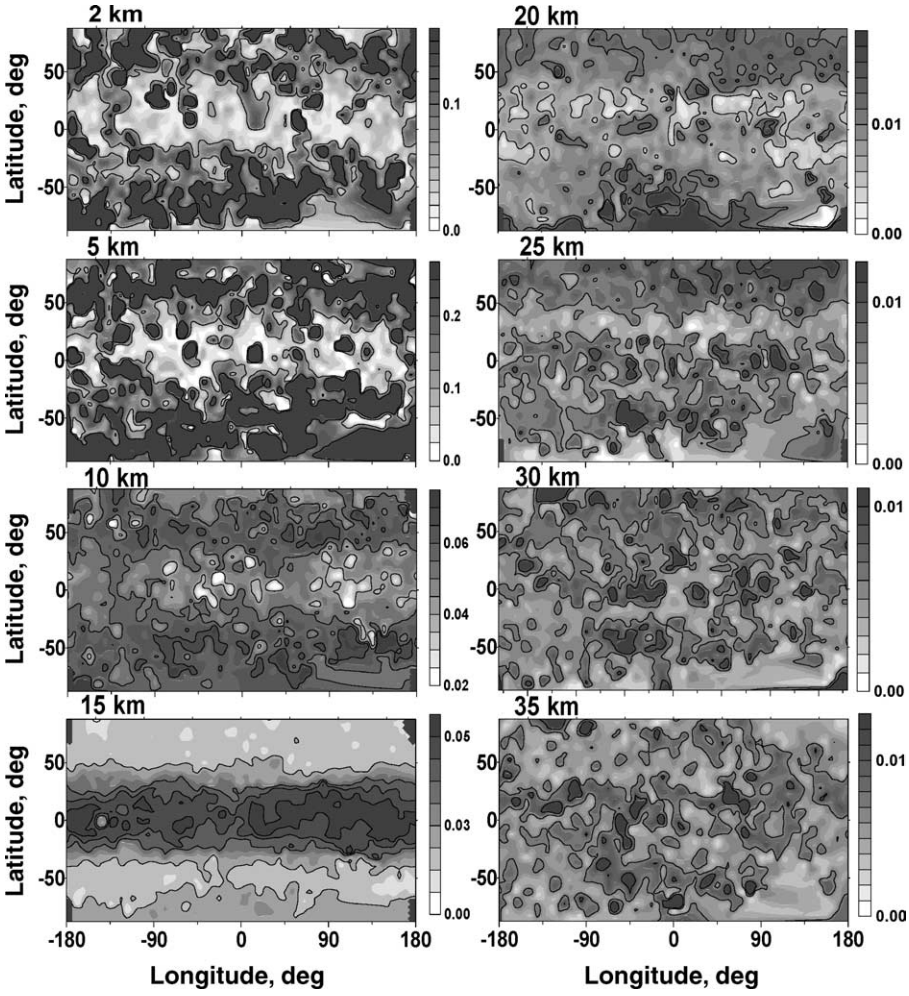

Fig. 6. Same as Fig. 3, but for July.

where we may expect increased IGW generation and intensity.

6. Conclusion

In this paper, an analysis of variances of the atmospheric dry temperature/refraction index from GPS/MET data is made. The variances may give information about global distributions of dynamically active regions, where we may expect increased meso-scale turbulence, IGW generation and wave intensity. Latitude–longitude distributions of the variances are different in different altitude layers. In January, at altitudes 2–5 km the refraction index variances have maxima in the middle and high latitudes and may reflect orographic peculiarities due to different distributions of mountain systems, oceans and continents. At altitude 10 km the maxima of the variances are concentrated between latitudes 20° and 60° in both northern and southern hemispheres and correlate with locations of tropospheric jet streams having maxima at altitudes 10–12 km. At altitudes 15–25 km the maxima exist at latitudes between −20° and 20° and related, probably, to deep convection and IGW generation in equatorial region. At 20–25 km the maxima of the refraction index are observed at high latitudes of northern hemisphere. At altitude 30 km absolute values of refraction index variances are smaller with lager variances in the northern hemisphere. The variances increase at 35 km, and the maxima near the equator appear.

In July, the variance distributions are generally similar to that in January at all altitudes except for a dominance of the variances in southern hemisphere above altitude of 20 km in July instead of the dominance in the northern hemisphere in January. The distributions of the refraction index variances in April and October are more symmetric than the winter and summer distributions.

The number of occultations obtained during the GPS/MET experiment provided only a few measurements near every horizontal grid point for each month

of year (see Section 3.3). Therefore, distributions of refractivity (dry temperature) in Figs. 3–6 are quite noisy. Further low-orbit GPS satellite observations are needed for accumulating larger databases and obtaining smoother three-dimension global distributions of mesoscale variability of the atmospheric refractivity and temperature.

Acknowledgements

This study was partly supported by the International Association for the promotion of cooperation with scientists from the New Independent States (INTAS) under grant INTAS-99-1186 and by the Russian Basic Research Foundation. The authors thank C. Rocken and S. Sokolovskiy for the supplying GPS/MET data and A. M. Gurvich for useful discussions.

References

Alexander, M.J., 1996. A simulated spectrum of convectively generated gravity waves. Propagation from the tropopause to the mesopause and effects on the middle atmosphere. J. Geophys. Res. 101, 1571–1588.

Alexander, M.J., 1998. Interpretations of observed climatological patterns in stratospheric gravity wave variance. J. Geophys. Res. 103, 8627–8640.

Alexander, M.J., Tsuda, T., Vincent, R.A., 2002. Latitudinal variations observed in gravity waves with short vertical wavelengths. J. Atmos. Sci. 59, 1394–1404.

Allen, S., Vincent, R., 1995. Gravity wave activity in the lower atmosphere: seasonal and latitudinal variations. J. Geophys. Res. 100, 1327–1350.

Eckermann, S., Hirota, I., Hocking, W., 1995. Gravity wave and equatorial wave morphology of the stratosphere derived from long-term rocket soundings. Quart. J. R. Meteor. Soc. 121, 149–186.

Eckermann, S., Preusse, P., 1999. Global measurements of stratospheric mountain waves from space. Science 286, 1534–1537.

Fetzer, E.J., Gille, J.C., 1994. Gravity wave variance in LIMS temperatures, part I: variability and comparison with background winds. J. Atmos. Sci. 51, 2461–2483.

Fritts, D.C., Alexander, M.J., 2003. A review of gravity wave dynamics and effects in the middle atmosphere. Rev. Geophys. 41 (1).

Gavrilov, N.M., Fukao, S., Hashiguchi, H, 1999. Multi-beam MU radar measurements of advective accelerations in the atmosphere. Geophys. Res. Lett. 26, 315–318.

Gavrilov, N.M., Richmond, A.D., Bertin, F., Lafeuille, M., 1994. Investigation of seasonal and interannual variations of internal gravity wave intensity in the thermosphere over Saint Santin. J. Geophys. 99, 6297–6306.

Gavrilov, N. M., Karpova, N. V., Jacobi, Ch., Gavrilov, A. N., 2004. Morphology of mesoscale refraction index variations in the tropo–stratosphere from GPS/MET satellite observations.J. Atmos. Solar-Terr. Phys. 66, accepted.

Hedin, A.E., 1991. Neutral atmosphere empirical model from the surface to lower exosphere MSISE-90, extension of the MSIS thermosphere model into the middle and lower atmosphere. J. Geophys. Res. 96, 1159–1172.

Hines, C.O., 1960. Internal atmospheric gravity waves at ionospheric heights. Can. J. Phys. 38, 1441–1481.

Hirota, I., 1984. Climatology of gravity waves in the middle atmosphere. J. Atmos. Terr. Phys. 46, 767–773.

Kursinski, E.R., Hajj, G.A., Schofield, J.T., Linfield, R.P., Hardy, K.R., 1997. Observing Earth's atmosphere with radio occultation measurements using the Global Positioning System. J. Geophys. Res. 102 (D19), 23429–23465.

McLandress, C., Alexander, M.J., Wu, D., 2000. Microwave limb sounder observations of gravity waves in the stratosphere: a climatology and interpretation. J. Geophys. Res. 105, 11947–11967.

Monin, A.S., Yaglom, A.M., 1971. Statistical Fluid Mechanics. MIT Press, Cambridge, MA.

Rocken, C., Athes, R., Exner, M., Hunt, D., Sokolovskiy, S., Ware, R., Gorbunov, M., Schreiner, W., Feng, D., Herman, B., Kuo, Y.-H., Zou, X., 1997. Analysis and validation of GPS/MET data in the neutral atmosphere. J. Geophys. Res. 102, 29849–29866.

Tsuda, T., Nishida, M., Rocken, C., Ware, R.H., 2000. A global morphology of gravity wave activity in the stratosphere revealed by the GPS occultation data (GPS/MET). J. Geophys. Res. 105, 7257–7274.

Ware, R., Rocken, C., Solheim, F., Exner, M., Schreiner, W., Anthes, R., Feng, D., Herman, B., Gorbunov, M., Sokolovskiy, S., Hardy, K., Kuo, Y., Zou, X., Trenberth, K., Meehan, T., Melbourne, W., Businger, S., 1996. GPS sounding of the atmosphere from low Earth orbit: preliminary results. Bull. Am. Meteorol. Soc. 77, 19–40.

Wu, D., Waters, J., 1996. Gravity-wave-scale temperature fluctuations seen by the UARS MLS. Geophys. Res. Lett. 23, 3289–3292.

Wu, D.L., Ao, C.O., Hajj, G.A., de la Torre Juarez, M., Mannucci, A.J., 2002. A study of sporadic E irregularities with SNR and phase measurements from GPS-LEO occultations. In: Abstracts of the 2002 CEDAR Meeting, Longmont, USA, 16–21 June. NCAR Press.